

Population of Isomeric States in Fusion and Transfer Reactions in Beams of Loosely Bound Nuclei near the Coulomb Barrier

N. K. Skobelev*

Joint Institute for Nuclear Research, ul. Joliot-Curie 6, Dubna, Moscow oblast, 141980 Russia

Received November 20, 2014

Abstract—The influence of the mechanisms of nuclear reactions on the population of ^{195m}Hg and $^{197m}\text{Hg}(7/2^-)$, ^{198m}Tl and $^{196m}\text{Tl}(7^+)$, and ^{196m}Au and $^{198m}\text{Au}(12^-)$ isomeric nuclear states obtained in reactions induced by beams of ^3He , ^6Li , and ^6He weakly bound nuclei is studied. The behavior of excitation functions and high values of isomeric ratios (σ_m/σ_g) for products of nuclear reactions proceeding through a compound nucleus and involving neutron evaporation are explained within statistical models. Reactions in which the emission of charged particles occurs have various isomeric ratios depending on the reaction type. The isomeric ratio is lower in direct transfer reactions involving charged-particle emission than in reactions where the evaporation of charged particles occurs. Reactions accompanied by neutron transfer usually have a lower isomeric ratio, which behaves differently for different direct-reaction types (stripping versus pickup reactions).

DOI: 10.1134/S1063778815050154

1. INTRODUCTION

For the first time, an isomeric state was discovered by Otto Hahn in 1921 in a ^{234}Pa nucleus formed in a uranium salt after the beta decay of the isotope ^{234}U . In 1935, such a state was observed in a ^{80}Br radioactive nucleus produced in the reaction $^{79}\text{Br}(n, \gamma)$. The first explanation for this phenomenon was given by Weizsäcker in 1936 [1]. More than 100 isomeric nuclear states of lifetime longer than 1 s have been found to date [2].

A feature that distinguishes an isomeric state of a nucleus from other excited states is that the probability for its transition to any other low-lying state is suppressed strongly by spin–parity selection rules. In particular, the deexcitation of a nucleus via high-multipolarity transitions (that is, transitions requiring a large change in the spin for going over to a lower lying state) and transitions characterized by a low transition energy is forbidden. The nuclear isomerism phenomenon was explained within the shell model of the nucleus. For odd nuclei in which the number of protons or neutrons is close to a magic number, this model predicted the existence of nuclear levels that are close in energy, but which differ substantially in spin.

There are several kinds of isomers [2]: shape isomers (decay is forbidden because of inconsistency of shapes), spin isomers (inconsistency of spins),

and K isomers (change in the spin orientation with respect to the symmetry axis of the nucleus being considered).

In the present study, we examine the population of isomeric states belonging to the class of spin isomers exclusively. For a specific nucleus, the ratio of the population probabilities for its ground and isomeric states, which is defined as σ_m/σ_g and which is referred to as the isomeric ratio (IR), depends on a number of factors—among other things, on the excitation energy of the nucleus formed in the reaction being considered and on the angular-momentum transfer l in the entrance reaction channel [3, 4]. Measurement of isomeric ratios in various nuclear reactions makes it possible to obtain important information both about the structure of the nucleus under study and about the degree of its excitation—in particular, about the distribution of the nuclear-level density and about the spins of excited nuclear states.

At the present time, much attention is given to studying reactions induced by weakly bound radioactive nuclei having unusual nuclear matter distributions, which have a strong effect on the interaction of nuclei. In the case of reactions involving loosely bound nuclei and nuclei that have a halo structure, it is natural to expect an increase in the mean angular momentum transfer in relation to reactions on densely packed nuclei (alpha particles and so on) because of a larger radius of nuclear-matter distribution in the projectile nucleus. This distribution may in turn change the population probabilities for isomeric

*E-mail: skobelev@jinr.ru

Table 1. Properties of the decay and spins of the isotopes under study in the ground and isomeric states

Nucleus— reaction product	$T_{1/2}$	J^π	E_γ , keV	I_γ , %
^{44g}Sc	3.927 h	2^+	1157.03	99.9
^{44m}Sc	58.6 h	6^+	271.13	86.7
^{196g}Tl	1.84 h	2^-	344.9	2
^{196m}Tl	1.41 h	7^+	505.2	6
			695.6	41
^{198g}Tl	5.3 h	2^-	675.9	11
^{198m}Tl	1.87 h	7^+	587.2	52
^{195g}Hg	9.9 h	$1/2^-$	779.80	7.0
^{195m}Hg	41.6 h	$13/2^+$	261.75	30.9
			560.27	7.0
^{197g}Hg	64.14 h	$1/2^-$	191.44	0.63
^{197m}Hg	23.8 h	$13/2^+$	133.99	33.0
^{196g}Au	6.183 h	2^-	332.983	22.9
			355.684	87
			426.0	7
$^{196m2}\text{Au}$	9.6 h	12^-	147.81	43
			168.37	7.6
			188.27	37.4
^{198m}Au	2.27 d	12^-	180.31	50
			204.10	40.8
			214.84	77

states of products of complete and incomplete fusion reactions and products of transfer reactions in relation to the population of the same states of the nuclei produced in reactions involving ordinary stable nuclei.

The influence of the structure of radioactive nuclei on fusion reactions in the region of threshold energies was explored in a number of experimental and theoretical studies. However, experimental data on the population of high spin states in reactions with such exotic nuclei are scanty.

The objective of the present study was to perform a further investigation into the effect of the mechanism of fusion and transfer reactions induced by the interaction of d and ^3He loosely bound nuclei, a ^6Li cluster nucleus, and a ^6He halo nucleus with light and heavy target nuclei on the excitation of formed nuclei, which led to the population of isomeric states

both in residual nuclei from evaporation reactions and in products of reactions involving the transfer of individual nucleons and clusters to a target or a projectile nucleus.

2. IMPLEMENTATION OF THE EXPERIMENTS

The experiments under discussion were performed in extracted ^3He beams from the U-120M cyclotron of the Nuclear Physics Institute, ASCR (Řež, Czech Republic), [5, 6] and in ^6He and ^6Li beams obtained at the DRIBs accelerator complex of the Joint Institute for Nuclear Research (JINR, Dubna). The details of the experiments and their results, including data on isomeric ratio, were amply described in [7, 8].

Target assemblies formed by scandium, gold, and platinum foils of different thickness (from 4 to 10 μm) and purity not poorer than 99% were installed on the path of accelerated ^3He ions at the center of reaction chamber. Platinum enriched in the isotope ^{194}Pt was deposited by an electrolytic method onto titanium foils 2.1 μm thick, and the such targets were also placed in the assemblies. A ^3He -beam intensity of up to $5 \times 10^{11} \text{ c}^{-1}$ was employed in the experiments. Beams of ^6Li and ^6He nuclei were obtained at the DRIBs (tandem of the U-400M and U-400 accelerators [9]) radioactive beam accelerator of the Laboratory of Nuclear Reaction at JINR. The maximum energy of the beam of accelerated ^6He ions was about 10 MeV per nucleon, and its intensity amounted to $5 \times 10^7 \text{ s}^{-1}$. The energy of the ^6Li and ^6He beams was measured by means of an MSP-144 magnetic spectrometer [7, 8].

After the completion of each irradiation run, the induced gamma activity was measured in all targets from ^{45}Sc , ^{197}Au , and ^{194}Pt . All of the measurements were performed with high-purity germanium (HPGe) detectors of efficiency 50% with respect to NaI ($3'' \times 3''$), their HWHM value being 1.8 keV at the photon energy of 1.3 MeV. The nuclides produced in the reactions under study were identified with allowance for the energies of their gamma decay and their lifetimes by using nuclear data compiled in [10].

The experiments being discussed involved measuring, over a broad energy range, the excitation functions for the Sc, Hg, Au, and Tl nuclei of our interest originating from various reactions in the ground and isomeric states (see Table 1). For the details concerning the implementation of the experiments and the calculation of cross sections for the production of various isotopes, the interested reader is referred to [5–8].

3. EXPERIMENTAL RESULTS AND THEIR ANALYSIS

3.1. Isomeric Ratios for ^{44}Sc

From the point of view of studying isomeric ratios, ^{44}Sc is an interesting nucleus lying near the $Z = 20$ and $N = 28$ shells. The half-lives with respect to gamma transitions from $^{44m}\text{Sc}(6^+)$ to $^{44g}\text{Sc}(2^+)$ and their intensities are convenient for measurements (see Table 1). The population of the ^{44m}Sc isomeric state and the isomeric ratios obtained in reactions induced by gamma rays and neutrons were analyzed in the review article of Mazur [11].

The excitation functions for the production of ^{44}Sc in the ground and isomeric states in reactions induced by deuteron and alpha-particle beams were measured in [12, 13]. An isomeric ratio smaller than unity was obtained for this isotope in the deuteron-induced reaction $^{45}\text{Sc}(d, t)^{44}\text{Sc}$. The isomeric ratio for ^{44}Sc in reactions with proton and alpha-particle beams [13, 14] has values of about two, which are higher than those in direct reactions of the (γ, p) and (d, α) types. The reaction $^{45}\text{Sc}(d, p2n)^{44g,m}\text{Sc}$ was recently studied in [15] at a deuteron energy higher than the Coulomb barrier for this reaction. A relatively large isomeric ratio value of about 1.5, which is characteristic of reactions proceeding through the formation of a compound nucleus, was also obtained in that study.

The excitation functions measured for the production of ^{44}Sc in the ground and isomeric states in the reaction $^{45}\text{Sc}(^3\text{He}, \alpha)^{44}\text{Sc}$ are given in Fig. 1, along with the calculated dependence of the isomeric ratio on the energy of ^3He bombarding particles [5, 16]. Particle-hole states formed upon the break of one neutron pair and the capture of one neutron are likely to be populated in reactions of this type that occur on nuclei in the vicinity of closed shells and which have positive Q values, in just the same way as in (d, α) reactions. The other nucleons remain with a high probability at their former levels in the nucleus. One can see that the isomeric ratio measured in this reaction for ^{44}Sc is lower than that in the fusion reactions considered above and, in the region above the reaction Coulomb barrier, undergoes virtually no change as the ^3He energy grows.

Thus, the above brief analysis of experimental results on the production of the isomer of ^{44}Sc in various reactions has led to the conclusion that the values of the isomeric ratio for ^{44}Sc and its behavior as the energy of bombarding particles grows depend greatly on the nuclear-reaction mechanisms (reactions proceeding through the formation of a compound nucleus versus direct transfer reactions).

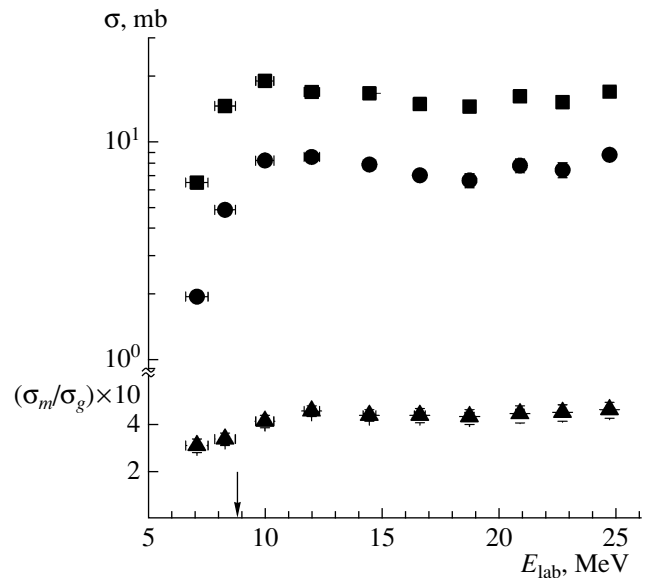


Fig. 1. Excitation functions for products of the reaction $^{45}\text{Sc}(^3\text{He}, \alpha)^{44}\text{Sc}$ (upper panel) and isomeric ratio for ^{44}Sc (lower panel) versus the ^3He energy: (closed boxes) $^{44g}\text{Sc}(2^+)$, (closed circles) $^{44m}\text{Sc}(6^+)$, and (closed triangle) σ_m/σ_g . The vertical arrow in this and the next figure indicates the energy of the Coulomb barrier.

3.2. Production of Isomers in Nuclei near the $Z = 82$ and $N = 126$ Shells in Beams of Loosely Bound and Radioactive Nuclei

3.2.1. Complete fusion reactions followed by the evaporation of neutrons and charged particles. We now proceed to consider the formation of nuclei in the ground and isomeric states near the $Z = 82$ and $N = 126$ shells. For target nuclei, we chose the spherical nuclei of gold and platinum.

In [6, 17], the isotope ^{198}Tl was obtained in the reaction $^{197}\text{Au}(^3\text{He}, 2n)^{198}\text{Tl}$ in the ground (2^-) and isomeric (7^+) states (see Fig. 2). The lower part of Fig. 2 gives the isomeric ratio for this isotope as a function of the energy of the ^3He beam. This isomeric ratio differs only slightly in magnitude from its counterpart for the same isotope ^{198}Tl produced in the reaction initiated by the bombardment of gold with alpha particles [18].

Figure 3 shows excitation functions for ^{198}Tl production in reactions where the fusion of gold with a ^6He loosely bound nucleus is followed by the evaporation of five neutrons: $^{197}\text{Au}(^6\text{He}, 5n)^{198}\text{Tl}$ [19]. From this figure, one can see that, as the energy of bombarding particles grows, the isomeric ratio increases, reaching a maximum value at an energy around 45 MeV and remaining, by and large, greater than unity over the whole energy range under study.

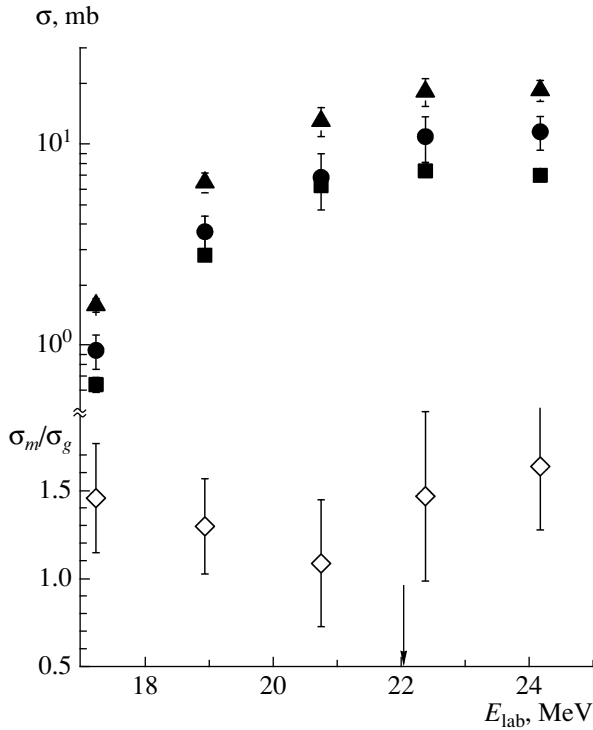


Fig. 2. Excitation functions for reactions leading to the production of ^{198}Tl (upper panel) and isomeric ratios for ^{198}Tl (lower panel) in the interaction of ^{197}Au with ^3He : (closed circles) $^{198m}\text{Tl}(7^+)$, (closed boxes) $^{198g}\text{Tl}(2^-)$, (closed triangles) $^{198(m+g)}\text{Tl}$, and (open diamonds) σ_m/σ_g .

At ^6He energies in excess of 50 MeV, the cross sections for the production of ^{196}Tl in the ground (2^-) and isomeric (7^+) states were also measured at two values of the energy, and the isomeric ratios were obtained for this nucleus (see Table 2). They do not differ from each other in magnitude and are close to the maximum value of the isomeric ratio for the isotope ^{198}Tl . It is noteworthy that the isomeric ratios obtained for the ^{196}Tl and ^{198}Tl nuclei are somewhat lower than the statistical-weight ratios $(2J_m + 1)/(2J_g + 1)$.

The isomeric ratios calculated for the ^{198}Tl nucleus on the basis of the statistical model for the decay of excited compound nuclei are represented by the solid and dashed curves in Fig. 3. In the calculations, use was made of the commonly accepted expressions for the dependence of the level density on the excitation energy and the orbital angular momentum l . This figure shows that, as the energy of bombarding particles increases, the experimental values of the isomeric ratio for ^{198}Tl grow in magnitude and exhibit nearly perfect agreement with the calculated values up to the maximum value of this ratio.

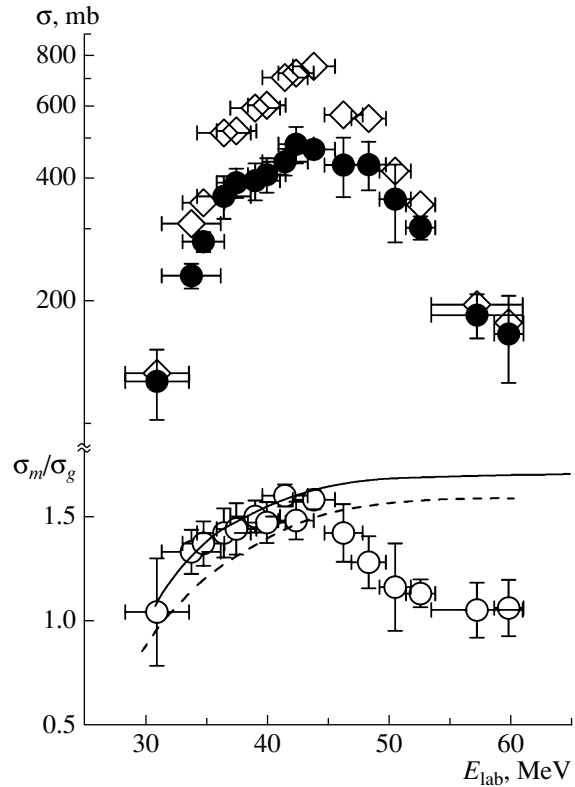


Fig. 3. Excitation functions for the reaction $^{197}\text{Au}(^6\text{He}, 5n)^{198}\text{Tl}$ of complete fusion followed by the evaporation of five neutrons (upper panel) and isomeric ratio for ^{198}Tl (lower panel) versus the energy of ^6He nuclei: (closed circles) $^{198g}\text{Tl}(2^-)$, (open diamonds) $^{198m}\text{Tl}(7^+)$, and (open circles) σ_m/σ_g . The solid and dashed curves represent the results obtained by calculating the isomeric ratio on the basis of the statistical model at various values of the spin-cutoff parameter σ (5.3 and 5, respectively).

For reactions with an alpha-particle beam that lead to the production of the same isotope ^{198}Tl , the isomeric ratio changes only slightly with increasing alpha-particle energy [18] and, in the energy range of 35–40 MeV, reaches a value barely different from the maximum value obtained in the beam of ^6He nuclei.

From the data that we obtained for the isomeric ratio for ^{198}Tl nuclei produced upon the $^6\text{He}+^{197}\text{Au}$ fusion reaction followed by neutron evaporation from

Table 2. Experimental cross sections for the population of the isomeric (σ_m) and ground (σ_g) states and σ_m/σ_g for the ^{196}Tl nucleus appearing as a product of the reaction $^{197}\text{Au}(^6\text{He}, 7n)$ at $E_{^6\text{He}} = 60$ and 57.4 MeV

$E_{\text{lab}}, \text{MeV}$	σ_m, mb	σ_g, mb	σ_m/σ_g
60 ± 1.2	549 ± 66	292 ± 65	1.88 ± 0.18
57.4 ± 3.7	465 ± 9	251 ± 55	1.85 ± 0.13

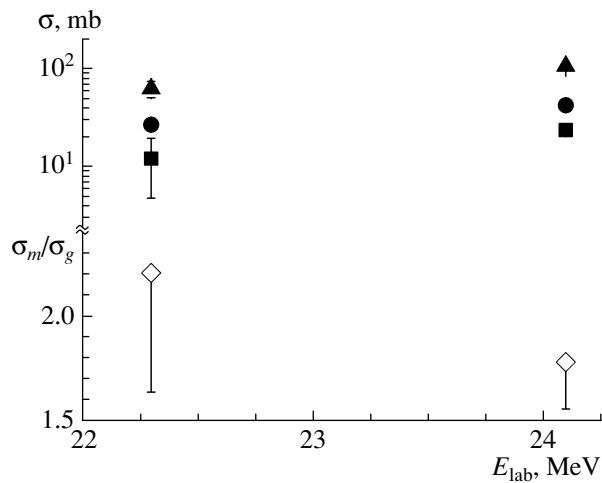


Fig. 4. Formation of $^{195m,g}\text{Hg}$ (upper panel) and isomeric ratio for ^{195}Hg (lower panel) in the interaction of ^{194}Pt with ^3He : (closed circles) $^{195m}\text{Hg}(13/2^+)$, (closed boxes) $^{195g}\text{Hg}(1/2^-)$, (closed triangles) $^{195(m+g)}\text{Hg}$, and (open diamonds) σ_m/σ_g .

the emerging compound nucleus, one can conclude that there are no substantial distinctions between the isomeric ratios in these reactions and reactions induced by alpha particles, even though the excitation energy of the compound nucleus is higher.

Indeed, the isomeric ratio obtained for ^{198}Tl in the $^{197}\text{Au}+^3\text{He}$ reaction (see Fig. 2) reaches values between 1.1 and 1.4, which are close to the isomeric-ratio values determined for ^{198}Tl produced in the fusion of alpha particles with ^6He —namely, $^{197}\text{Au}(^4\text{He}, 3n)$ [18] and $^{197}\text{Au}(^6\text{He}, 5n)$ [19].

In [20], the excitation functions were measured for the production of ^{195}Hg in the ground and isomeric states in the reaction $^{197}\text{Au}(p, 3n)^{195m,g}\text{Hg}$, where the isomeric ratio (see Fig. 1 in [20]) was also greater than unity. The isomeric ratios for the production of the isotopes ^{195}Hg and ^{197}Hg in fusion reactions induced by proton and deuteron beams were calculated in [21] on the basis of the EMPIRE-3, TENDL(2010), and TALYS-1.26 codes. Those calculations led to a relatively good agreement with experimental data.

In bombarding ^{194}Pt nuclei with ^3He loosely bound stable nuclei, the isotope ^{195}Hg in the ground and isomeric states was produced in the reaction $^{194}\text{Pt}(^3\text{He}, 2n)^{195}\text{Hg}$ (see Fig. 4) [6, 17]. The isomeric ratio value that we obtained for this isotope is close to the analogous values observed for it in the aforementioned reactions proceeding through the compound nucleus that are induced by proton and deuteron beams [20, 21].

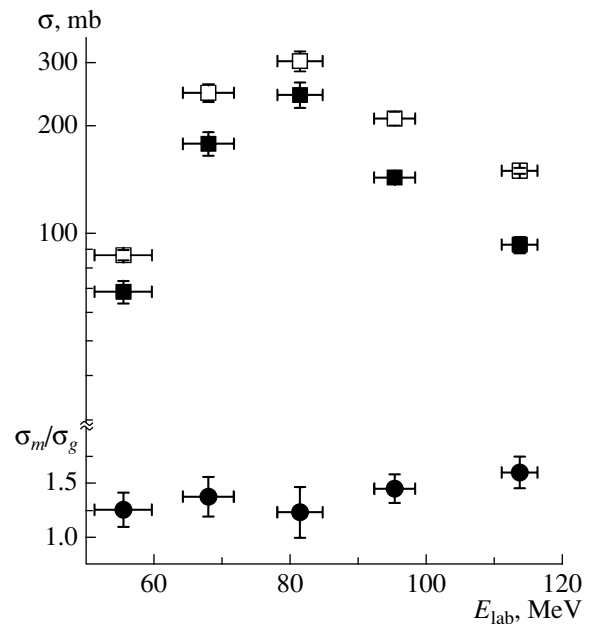


Fig. 5. Cross section for the production of the isotope ^{195}Hg (upper panel) and isomeric ratio for ^{195}Hg (lower panel) for the $^6\text{He}+^{197}\text{Au}$ reaction versus the ^6He energy: (closed boxes) $^{195g}\text{Hg}(1/2^-)$, (open boxes) $^{195m}\text{Hg}(13/2^+)$, and (closed circles) σ_m/σ_g .

3.2.2. Reactions involving the evaporation of charged particles. The population of the isomeric state in the ^{195}Hg nucleus (see Fig. 5) synthesized in the reaction $^{197}\text{Au}(^6\text{He}, p7n)^{195}\text{Hg}$ was also observed at higher energies of ^6He bombarding particles [22]. The form of the excitation function and a comparison of experimental cross sections with their calculated counterparts indicate that this reaction channel is indeed that of the deexcitation of a compound nucleus via the evaporation of a charged particle (proton) and seven neutrons.

The production of the isotope ^{197}Hg and the population of the ground and isomeric states in it was studied in reactions induced by photon, neutron, and proton beams [23, 24] and reactions induced by triton beams [25]. In those studies, it was found that the isomeric ratio in the reactions in question ranges between 0.04 and 3.5.

We have also measured the isomeric ratio [6, 17] for the isotope ^{197}Hg produced in the $^{197}\text{Au}+^3\text{He}$ reaction (see Fig. 6). In this reaction, the isomeric ratio has a relatively small value of about 0.1, which changes only slightly in response to a change in the energy of the ^3He beam. A calculation of the cross section for the production of ^{197}Hg shows that this isotope originates most likely from the exchange reaction $^{197}\text{Au}(^3\text{He}, t)^{197m,g}\text{Hg}$ rather than from the

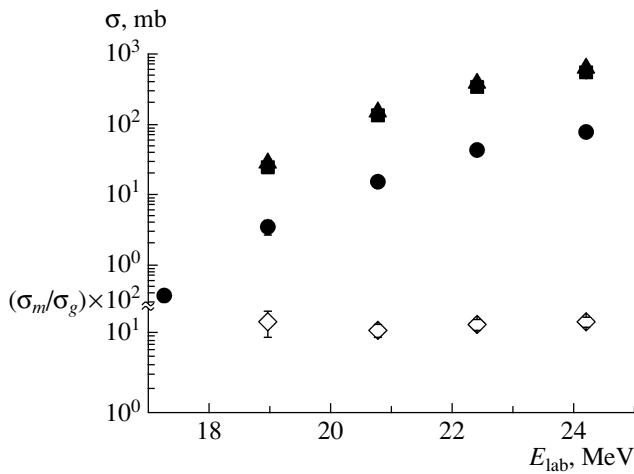


Fig. 6. Excitation functions for reactions leading to $^{197m,g}\text{Hg}$ production (upper panel) and isomeric ratio for ^{197}Hg (lower panel) in the interaction of ^{197}Au with ^3He : (closed boxes) $^{197g}\text{Hg}(1/2^-)$, (closed circles) $^{197m}\text{Hg}(13/2^+)$, (closed triangles) $^{197(m+g)}\text{Hg}$, and (open diamonds) σ_m/σ_g .

respective (^3He , $p2n$) fusion reaction involving the emission of a charged particle.

3.2.3. Reactions proceeding via nucleon and clusters transfer. The population of isomeric states in the gold isotopes ^{196}Au and ^{198}Au at energies in the vicinity of the reaction barriers is of great interest; these states have higher spins of $J^\pi = 12^-$ (see Table 1). The isotopes ^{196}Au and ^{198}Au were produced in reactions induced by proton, deuteron, and alpha-particle beams. The isomeric ratio was measured for the isotope ^{196}Au produced in the deuteron- and triton-induced reactions $^{197}\text{Au}(d, t)$ and $^{197}\text{Au}(t, tn)$, and their values were found to be low [25], which is likely to indicate that direct reactions make a dominant contribution to the production of this gold isotope.

The isomeric ratios for ^{196}Au in the reaction $^{193}\text{Ir}(\alpha, n)^{196}\text{Au}$ induced by an alpha-particle beam were measured in [4, 26], the data on the isomeric-ratio values in the region of energies near the reaction barrier from those two studies being different by nearly an order of magnitude. It is noteworthy that the data from [26] on the isomeric ratio for ^{196}Au agree with the results of the calculations on the basis of the EMPIRE-2.6 code for reactions proceeding through the formation of a compound nucleus.

The probability for the excitation of the $J^\pi = 12^-$ state should increase in fusion reactions involving heavy ions and proceeding via high orbital-angular-momentum transfers. Indeed, it was shown that, for the isotope ^{196}Au produced in the $^{192}\text{Os}(^{11}\text{B}$,

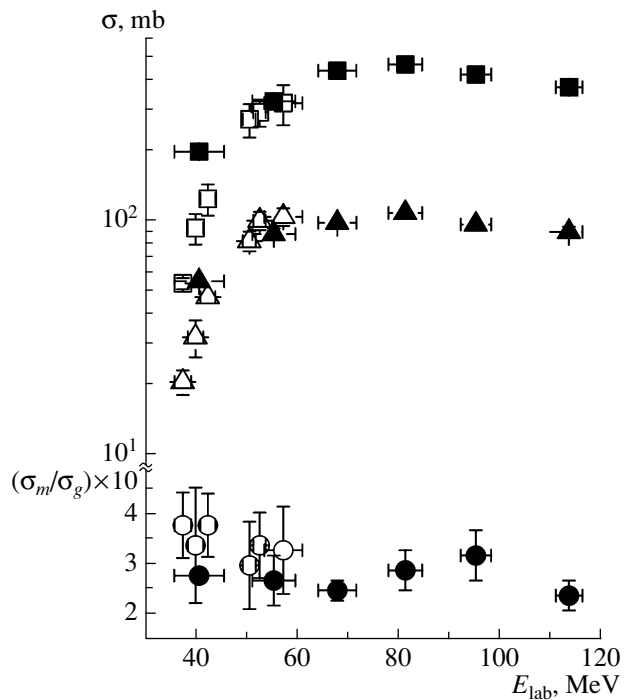


Fig. 7. Excitation functions for the stripping of one neutron in $^6\text{He}-^{197}\text{Au}$ interaction leading to the production of ^{196}Au (upper panel) and change in the isomeric ratio in response to the growth of the ^6He energy: (closed and open boxes) $^{196g}\text{Au}(2^-)$, (closed and open triangles) $^{196m}\text{Au}(12^-)$, and (closed and open circles) σ_m/σ_g .

$\alpha 3n)^{196}\text{Au}$ reaction, the isomeric ratio grows from 1.7×10^{-2} at the average orbital-angular-momentum transfer of $l = 3$ to 3×10^{-1} at $l = 15$ in the region of energies near the Coulomb barrier [27]. However, the isomeric ratio for ^{196}Au in this reaction inclusive, which involves the emission of a charged particle, has a relatively low value even in relation to the isomeric-ratio value obtained in the fusion reaction induced by an alpha-particle beam [26].

Let us now consider the population of isomeric states in ^{196}Au and ^{198}Au nuclei formed in reactions of few-nucleon transfer. Figure 7 shows the excitation functions for the isotope ^{196}Au produced in the ground and isomeric states upon the interaction of ^6He with a ^{197}Au target nucleus [19, 22]. The lower part of this figure gives the isomeric ratio σ_m/σ_g obtained for ^{196}Au in this reaction in two experiments at different energies of ^6He beams. Over the whose measured range of energies, the isomeric ratio in question changes only slightly with increasing energy and is larger in magnitude than the isomeric ratio obtained in the same study for the ^{198}Au isotope. Collisions between ^6He and gold nuclei are accompanied

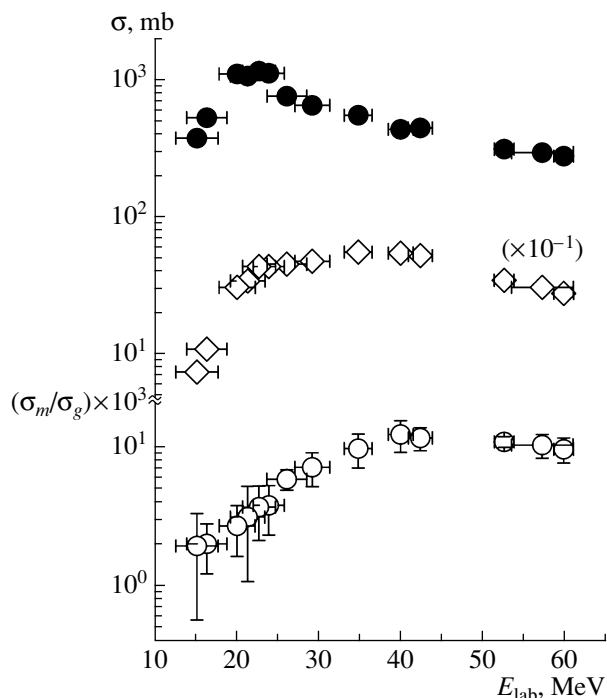


Fig. 8. Excitation function for neutron pickup in ${}^6\text{He}-{}^{197}\text{Au}$ interaction leading to ${}^{198}\text{Au}$ formation (upper panel) and change in the isomeric ratio (lower panel) in response to an increase in the ${}^6\text{He}$ energy: (closed circles) ${}^{198g}\text{Au}(2^-)$, (open diamonds) ${}^{198m}\text{Au}(12^-)$, and (open circles) σ_m/σ_g .

by sizable energy transfers leading to the excitation of external orbits and to the breaking of neutron pairs that is followed by the emission of one of the neutrons. For nuclei in the vicinity of closed shells, this results in the formation and population of excited particle-hole states, including isomeric states. The population probability for excited states grows with increasing energy of bombarding particles. This approach to the formation and population of particle-hole states is considered within the shell and exciton models.

The cross sections for reactions leading to the production of the isotope ${}^{196}\text{Au}$ in the ground and isomeric states were also measured in ${}^3\text{He}$ and alpha-particle beams [6, 18]. As the ${}^3\text{He}$ -beam energy changes, the resulting isomeric ratios behave in just the same way as in reactions induced by ${}^6\text{He}$ beams; that is, they undergo virtually no changes as the particle energy grows above the Coulomb barrier. The absolute values of the isomeric ratios have the largest values in reactions with ${}^6\text{He}$.

The production of ${}^{198}\text{Au}$ in the ground and isomeric states was studied earlier in neutron transfer to ${}^{197}\text{Au}$ nuclei in the interaction with deuterons [25] and alpha particles [18], in which case the growth

of the isomeric ratio with increasing energy was observed; also, relatively low values of the isomeric ratio (10^{-3} – 10^{-2}) were obtained.

In Fig. 8, the excitation functions for the production of the isotope ${}^{198}\text{Au}$ in the ground and isomeric states in transfer reactions induced by ${}^6\text{He}+{}^{197}\text{Au}$ interaction are given along with the isomeric ratio σ_m/σ_g calculated for this isotope in [19]. One can see that the production of ${}^{198}\text{Au}$ is much less probable in the isomeric state than in the ground state. The shape of the excitation functions for ${}^{198}\text{Au}$ production is also indicative of ${}^{198m}\text{Au}$ and ${}^{198g}\text{Au}$ formation in direct reactions.

A possible explanation for a low isomeric ratio value is that the neutron transferred from a light nucleus to a heavy gold target nucleus populates in it low-lying states similar to states of the projectile nucleus [27], and this cannot help affecting the population of high-lying isomeric states (12^-) in the ${}^{198}\text{Au}$ nucleus formed. As the projectile energy grows, the probability for the population of ever higher excited states naturally increases, and so do the isomeric ratio together with it.

The population of isomeric states in ${}^{198}\text{Au}$ was also studied in other transfer reactions involving halo nuclei. Neutron transfer to a ${}^{197}\text{Au}$ target nucleus from a ${}^8\text{He}$ projectile nucleus was observed with a high probability [28]. In that reaction, the isomeric ratio for ${}^{198}\text{Au}$ grows in the subbarrier region but thereupon reaches a plateau around a value of 10^{-2} .

As was shown in [8, 29, 30], the probability for deuteron transfer from a ${}^6\text{Li}$ nucleus is high near the reaction Coulomb barrier. In just the same way as in reactions on Pt involving deuterons, there occurs the population of isomeric states in ${}^{198}\text{Au}$, the isomeric ratio for ${}^{198}\text{Au}$ in the reaction with ${}^6\text{Li}$ reaching somewhat greater values of about 10^{-1} [31]. In the ${}^{209}\text{Bi}+{}^6,{}^7\text{Li}$ reactions [32], the isomeric ratio was measured upon the capture from ${}^6\text{Li}$ and ${}^7\text{Li}$ of both an alpha particle and d or t , respectively, with the production of the isomers of ${}^{212}\text{At}$ and ${}^{211}\text{Po}$. The $\alpha+{}^{209}\text{Bi}$ and $\alpha+{}^{208}\text{Pb}$ fusion reactions leading to the production of the same nuclei were explored for the purposes of calibration. In the same study, it was shown that, in the capture of an alpha particle from lithium, the isomeric ratio as a function of the lithium energy has a more gently sloping shape and, at the maximum, is close to but somewhat higher than the reference isomeric-ratio value obtained in the reactions induced by alpha particles. In the case of triton capture from ${}^7\text{Li}$ and the production of the isomer ${}^{211m}\text{Po}$, the isomeric ratio has a relatively high value (about 10^{-1} , in just the same way as the

isomeric ratio for ^{198}Au in the reaction induced by ^6Li [31]), which undergoes virtually no changes as the ^7Li energy grows.

4. DISCUSSION

Investigation of nuclear reactions with beams of accelerated ions with an energy of near the reaction barrier shows that the behavior of cross sections for fusion and transfer reactions depends greatly on the reaction Q_{gg} value. At positive values of Q_{gg} , a compound nucleus that arises in reactions involving loosely bound and halo nuclei has a higher excitation energy, and the cross sections for $2n$ -evaporation reaction channels are relatively large in the subbarrier energy region [8]. By and large, however, a positive Q value in fusion reactions has virtually no effect on the behavior and absolute values of isomeric ratios (isomeric ratios grow in the subbarrier region, thereupon reaching a plateau).

The population of ground and isomeric states of nuclei originating from fusion reactions depends on the excitation energy of the compound nucleus and on the maximum value and distribution of the orbital angular momentum transfer l , as well as on the sort of particles emitted in the deexcitation of the nucleus that are able to carry away various energies and angular momenta. If the bombarding-particle energy is sufficiently high for the levels that have various spin values possible for the compound nucleus to be populated, then the isomeric ratio should tend to the limit of the ratio $(2J_m + 1)/(2J_g + 1)$ from the statistical approach to the population process.

In order to calculate isomeric ratios for products of incomplete fusion and nucleon transfer reactions, it is necessary to make an assumption on the orbital angular momentum (l) and energy transfers from a particle or a cluster in the entrance channel. It is probable that low-lying single-particle levels in the newly formed nucleus are populated in the case of transfer of particles that have a low energy and a low orbital angular momentum. This will reduce substantially the number of steps of deexcitation of this nucleus and diminish the population of isomeric states.

A strong dependence of the cross sections for transfer reactions on the reaction Q value stems from the need for preserving the distance of closest approach prior to and after nucleon transfer and from the conservation of the total energy. This results, among other things, in selecting, among all values of the primary-channel energy in the interaction of nuclei, an optimum positive value that is close or equal to Q_{gg} and which may lead to the depopulation of external orbits of the projectile as it propagates in the target field [33]. This circumstance should lead to

an enhanced probability for neutron transfer from the target nucleus [27, 33].

In the case of charged particle transfer, the change in the energy should be corrected not only with allowance for the difference of Q_{gg} but also with allowance for the change in the Coulomb interaction energy [27, 34]; therefore, there is an effective change in the energy—that is, $E_{\text{eff}} = Q_{gg} - Q_{\text{opt}}$, where the second term stems from the change in the Coulomb energy. The excitation energy associated with nucleon transfers can roughly be estimated as $E^* = E_{\text{eff}}$ [35].

For light projectile and target nuclei, the charges are close, while the change in the energy E_i in the entrance reaction channel near the Coulomb barrier is bounded. As a result, Q_{opt} usually changes from 0 to 1 MeV both for neutron and for proton transfer [34]. This should lead to a predominant population of the ground and low-lying states in the final nucleus.

The change in the energy is especially sizable in the case of proton transfer from light projectiles to heavy target nuclei; it may reach a value of about 10 MeV. The change in the energy upon proton transfer is related to the quantity

$$Q_{\text{opt}} = E_i \left[\frac{Z_f z_f}{Z_i z_i} - 1 \right],$$

where E_i is the projectile energy in the c.m. frame and Z_i and z_i (Z_f and z_f) are the charge numbers of participant nuclei in the reaction entrance (exit) channel [33]. For example, Q_{opt} may reach a value in excess of 6 MeV upon proton and deuteron transfer from a ^6Li light projectile nucleus to a ^{209}Bi target nucleus. This also entails the circumstance that a charged particle is transferred from a projectile nucleus to highly excited states of a heavy target nucleus.

Measurement of the isomeric ratio in the reaction $^{197}\text{Au}(^3\text{He}, X)^{197}\text{Hg}$ led to a relatively high value of about 0.1, which undergoes virtually no change in response to the change in the ^3He energy. This result indicates that the proton–neutron exchange reaction or proton transfer proceeds predominantly to highly excited states of the target nucleus [27].

The cross sections for the $^3,^6\text{He}+^{197}\text{Au}$ reactions involving neutron transfer both to a target nucleus and to a projectile nucleus were recently calculated, along with the excitation energy of the residual nucleus, on the basis of solving the time-dependent Schrödinger equation for the matrix of coupling of two-center neutron channels by means of an expansion in Bessel functions [36, 37]. These estimates of cross sections for transfer reactions and of the excitation energy are compatible with the above assumptions concerning the population of various excited

states upon neutron transfer from a light projectile nucleus (^3He and ^6He) and from a heavy target.

5. CONCLUSIONS

A comparison of the cross sections measured for the production of Hg, Tl, and Au nuclei in the ground and isomeric states [^{195m}Hg and $^{197m}\text{Hg}(7/2^-)$, ^{198m}Tl and $^{196m}\text{Tl}(7^+)$, and ^{196m}Au and $^{198m}\text{Au}(12^-)$] in reactions induced by beams of ^3He , ^6He , and ^6Li loosely bound nuclei and other stable nuclei and the isomeric ratios calculated for them makes it possible to associate more reliably these isomeric ratios with the mechanisms of nuclear reactions and with basic factors affecting them (specifically, with orbital-angular-momentum transfers from particles in the entrance reaction channel and with the probability for the population of high-spin levels in product nuclei).

The behavior of excitation functions and isomeric ratios for products of fusion reactions involving neutron emission can be explained within models of nuclear reactions proceeding through a compound nucleus. Such reactions are usually characterized by higher isomeric ratios that change with particle energy (owing to changes in the orbital-angular-momentum transfer and in the excitation energy).

A comparison of experimental values obtained for isomeric ratios in different reactions shows that there is a large difference in the values and the behavior of the isomeric ratios between fusion and direct reactions. Reactions involving the emission of charged particles may have different isomeric ratios for different reaction types. In particular, the isomeric ratio in direct reactions is usually low.

Isomeric ratios are usually lower in direct reactions proceeding via neutron transfer to a target nucleus or a projectile particle (stripping or pickup reactions). Population of low-lying states occurs upon neutron transfer from a light projectile nucleus to a heavy target nucleus, and the probability for the population of high-lying states grows with increasing energy of bombarding particles. In this case, the isomeric ratio in the subbarrier region and near the Coulomb barrier grows with the energy of bombarding particles.

In reactions where a light projectile picks up a neutron from a target nucleus, this neutron leaves a vacancy (hole) at the level that it originally occupied in the target nucleus. Excited particle-hole and isomeric states may be populated upon filling this vacancy. As a rule, reactions involving the pickup or knockout of one of the target nucleons proceed at a higher excitation energy and have smaller cross-section values. Although the cross section for nucleon capture from the target nucleus grows as the energy of bombarding particles and the probability

for the formation of high-lying excited particle-hole states in the final nucleus increase, the isomeric ratio for such reactions is virtually independent of the bombarding-particle energy.

ACKNOWLEDGMENTS

I am grateful to my colleagues with whom I performed experiments devoted to measuring cross sections for the production of the nuclei studied here and the isomeric ratios for them in the aforementioned reactions induced by ^3He , ^6He , and ^6Li beams obtained at the accelerators of Nuclear Physics Institute (ASCR, Řež, Czech Republic) and JINR (Dubna, Russia).

REFERENCES

1. C. F. von Weizsäcker, *Naturwissenschaften* **24**, 813 (1936).
2. P. Walker and G. Dracoulis, *Nature* **399**, 35 (1999).
3. D. E. DiGregorio, K. T. Lesko, B. A. Harmon, et al., *Phys. Rev. C* **42**, 2108 (1990).
4. V. Yu. Denisov, V. A. Zheltonozhskii, and S. V. Reshit'ko, *Phys. At. Nucl.* **56**, 57 (1993).
5. N. K. Skobelev, A. A. Kulko, Yu. E. Penionzhkevich, et al., *Phys. Part. Nucl. Lett.* **10**, 410 (2013).
6. N. K. Skobelev, Yu. E. Penionzhkevich, E. I. Voskoboynik, et al., *Phys. Part. Nucl. Lett.* **11**, 114 (2014).
7. Yu. E. Penionzhkevich et al., *Eur. Phys. J. A* **31**, 185 (2007).
8. Yu. E. Penionzhkevich, S. M. Lukyanov, R. A. Astabatyanyan, et al., *J. Phys. G* **36**, 025104 (2009).
9. Yu. Ts. Oganessian and G. G. Gulbekian, in *Proceedings of the International Conference Nuclear Shells—50 Years*, Ed. by Yu. Ts. Oganessian and R. Kalpakchieva (World Scientific, Singapore, 2000), p. 61.
10. S. Y. F. Chu, L. P. Ekstöm, and R. B. Firestone, *The Lund/LBL Nuclear Data, Search Version (1999)*; <http://nucldata.nuclear.lu.se/nucldata/toi/>
11. V. M. Mazur, *Phys. Part. Nucl.* **31**, 188 (2000).
12. K. L. Chen and J. M. Miller, *Phys. Rev. B* **134**, 1269 (1964).
13. T. Matsuo, J. M. Matuszek, Jr., N. D. Dudley, and T. T. Sugihara, *Phys. Rev.* **139** B886 (1965).
14. E. A. Bogila, V. I. Gavriluk, and V. A. Zheltonozhskii, *Bull. Acad. Sci. USSR: Phys.* **55**, 48 (1991).
15. A. Hermanne et al., *Nucl. Instrum. Methods Phys. Res. B* **270**, 106 (2012).
16. N. K. Skobelev, A. A. Kulko, Yu. E. Penionzhkevich, et al., *Bull. Russ. Acad. Sci. Phys.* **77**, 795 (2013).
17. E. I. Voskoboynik, N. K. Skobelev, Yu. E. Penionzhkevich, et al., *Bull. Russ. Acad. Sci.: Phys.* **78**, 361 (2014).
18. N. Chakravarty, P. K. Sarkar, and S. Ghosh, *Phys. Rev. C* **45**, 1171 (1992).
19. A. A. Kulko, N. A. Demekhina, R. Kalpakchieva, et al., *J. Phys. G* **34**, 2297 (2007).

20. Y. Nagame et al., Phys. Rev. C **41**, 889 (1990).
21. M. Sadeghi et al., Phys. Rev. C **85**, 034605 (2012).
22. N. K. Skobelev, Yu. E. Penionzhkevich, A. A. Kulko, et al., Phys. Part. Nucl. Lett. **10**, 248 (2013).
23. R. Vandenbosch and J. R. Huizenga, Phys. Rev. **120**, 1313 (1960).
24. S. Sudár, and S. M. Qaim, Phys. Rev. C **73**, 034613 (2006).
25. V. R. Casella, Report LA-5830-T (Los Alamos Scientific Laboratory, 1975).
26. T. V. Chuvil'skaya, Yu. G. Seleznev, A. A. Shirokova, and M. German, Bull. Russ. Acad. Sci.: Phys. **63**, 825 (1999).
27. R. A. Broglia and A. Winter, *Heavy Ion Reactions*, Lecture Notes, Vol. 1 (Addison-Wesley, Redwood City, USA, 1991), p. 349.
28. A. Lemasson, A. Navin, M. Rejmund, et al., Phys. Lett. B **697** 454 (2011).
29. Yu. E. Penionzhkevich et al., Int. J. Mod. Phys. E **17**, 2349 (2008).
30. N. K. Skobelev, N. A. Demekhina, R. Kalpakchieva, et al., Phys. Part. Nucl. Lett. **6**, 208 (2009).
31. A. Shrivastava, A. Navin, A. Lemasson, et al., Phys. Rev. Lett. **103**, 232702 (2009).
32. L. R. Gasques, M. Dasgupta, D. J. Hinde, et al., Phys. Rev. C **74**, 064615 (2006).
33. W. R. McMurray et al., Nucl. Phys. A **265**, 517 (1976).
34. P. J. A. Buttle and L. J. B. Goldfarb, Nucl. Phys. A **176**, 299 (1971).
35. A. Shrivastava, A. Navin, A. Diaz-Torres, et al., Phys. Lett. B **718**, 931 (2013).
36. V. V. Samarin and K. V. Samarin, Bull. Russ. Acad. Sci.: Phys. **76**, 450 (2012).
37. V. V. Samarin, in *Proceedings of the 7th International Symposium on Exotic Nuclei (EXON-2014), Kaliningrad, Russia, Sept. 8–13, 2014* (JINR, Dubna, 2014), p. 30.